Zeitschrift: IABSE congress report = Rapport du congrès AIPC = IVBH Kongressbericht

Band: 3 (1948)

Rubrik: IVb: Continuous slabs

IVb1

Calcul approché des dalles rectangulaires en béton armé pour une charge uniformément répartie ou hydrostatique

Näherungsmethode zur Berechnung von rechteckigen Platten aus Eisenbeton bei gleichmässig verteilter und hydrostatischer Belastung

Approximative method of analysis for rectangular reinforced concrete plates under uniformly distributed or hydrostatic load

PROF. IR. P. P. BIJLAARD
Technische Hoogeschool Delft, Technical adviser I. A. B. S. E.

Introduction

As a direct integration of the differential equation of the plate is in general not possible for rectangular plates, supported at the edges, several methods have been developed to cope with this difficulty, using double and single Fourier series, differences equations, etc. Some of these methods lead to sufficiently accurate results. They are, however, rather laborious, especially if all kinds of boundary conditions have to be taken into account, whilst no usable general formulae for bending moments, etc. are obtained. It is true Marcus (1) gave relatively simple formulae for rectangular plates with uniformly distributed load, but these have not been derived directly. They have been composed in such a manner that they approximate as much as possible the results of his more accurate calculation (2), which leads only to numerical results.

At the other hand our method (3) is rather simple and gives a clear insight in the way in which the plates carry the load. Moreover it leads

---

(1) MARCUS, *Die vereinfachte Berechnung biegsamer Platten*, Springer, Berlin, 1925.
(2) MARCUS, *Die Theorie elastischer Gewebe und ihre Anwendung auf die Berechnung biegsamer Platten*, Springer, Berlin, 1924.
(3) BIJLAARD, *De Ingenieur*, n° 26, 1934, n° 23, 1935; *De Ingenieur in Ned. Indië*, n° 12, 1935; *Proc. Third Engineering Congress*, Tokio, 1936.

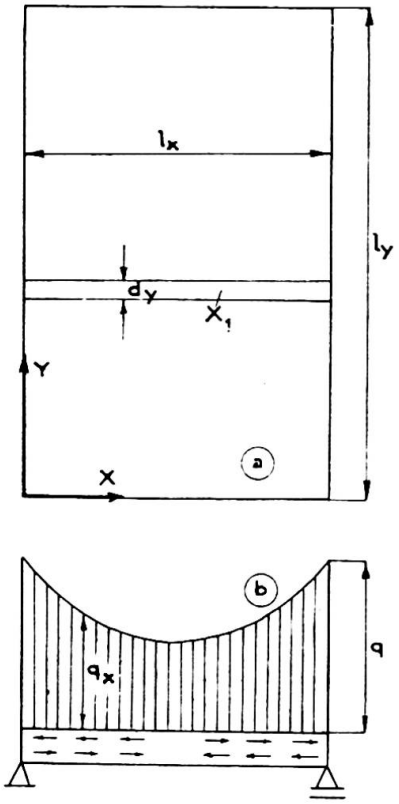

Fig. 1.

to simple general formulae for the maximum bending moments as functions of the ratio $\varepsilon = l_y/l_x$ of the sides, which are similarly built for all boundary conditions, for uniformly distributed as well as for hydrostatic load. Furthermore our formulae are more accurate than those of Marcus.

Simply supported plates

Let us consider first a rectangular plate (fig. 1*a*) with simply supported edges, carrying an arbitrary load $q = f(x, y)$. An arbitrary X-strip, X_1, of this plate, having a breadth dy, will only have to carry a vertical load q_x, the remainder of the load q being carried by the vertical shearing forces acting on its sides. The bending moment per unit breadth of the strip, due to this vertical load q_x, we denote by M_{xv}.

As, however, also twisting moments M_{yx} and $M_{yx} + \frac{\partial M_{yx}}{\partial y} dy$ are acting on the sides of the strip, which cause bending moments $M_{x\tau}$ per unit breadth of its cross sections, the real bending moment per unit breadth of the strip amounts to

$$M_x = M_{xv} + M_{x\tau} \tag{1}$$

so that

$$M_{xv} = M_x - M_{x\tau} \tag{2}$$

We know that (4)

$$M_x = -D\left(\frac{\partial^2 w}{\partial x^2} + \nu \frac{\partial^2 w}{\partial y^2}\right) \tag{3}$$

(4) TIMOSHENKO, *Theory of Plates and Shells*, 1940, p. 88.

whilst

$$M_{yx} = -D(1-\nu)\frac{\partial^2 w}{\partial x \partial y}$$

acting on strip X_1 as indicated in fig. 1*b*. Consequently the total moment exercised per unit length of the strip by the twisting moments M_{yx} and $M_{yx} + \frac{\partial M_{yx}}{\partial y} dy$ is

$$\frac{\partial M_{yx}}{\partial y} dy = -D(1-\nu)\frac{\partial^3 w}{\partial x \partial y^2} dy$$

acting on the strip in the opposite direction of the arrows in fig 1*b*. Hence the bending moment M_{xx} per unit breadth of the strip, caused by the twisting moments, amounts to

$$M_{xx} = -D(1-\nu)\int_x^{l_x} \frac{\partial^3 w}{\partial x \partial y^2} dx = -D(1-\nu)\left[\frac{\partial^2 w}{\partial y^2}\right]_x^{l_x} = D(1-\nu)\frac{\partial^2 w}{\partial y^2} \tag{4}$$

a similar result being already obtained by Marcus.

But with eqs. (3) and (4) it follows now from eq. (2) that

$$M_{xv} = -D\left(\frac{\partial^2 w}{\partial x^2} + \frac{\partial^2 w}{\partial y^2}\right) \tag{5}$$

whence we obtain, by changing x and y

$$M_{yv} = -D\left(\frac{\partial^2 w}{\partial x^2} + \frac{\partial^2 w}{\partial y^2}\right) \tag{6}$$

so that we draw the conclusion that

$$M_{xv} = M_{yv}\,. \tag{7}$$

Hence at any point of a rectangular plate with simply supported edges and arbitrary load, the bending moment M_{xv} per unit breadth, that would occur in an X-strip, if it had to carry its total vertical load q_x as a simple beam, without being discharged by the twisting moments M_{yx}, is equal to the bending moment M_{yv}, occurring at the same point in an Y-strip, if it would have to carry its total vertical load q_y as a simple beam, whilst of course

$$q_x + q_y = q\,. \tag{8}$$

At the other hand we know that, according to eq. (3), whence M_y follows by changing x and y, we have

$$M_x + M_y = -D(1+\nu)\left(\frac{\partial^2 w}{\partial x^2} + \frac{\partial^2 w}{\partial y^2}\right) \tag{9}$$

so that it follows from eqs. (5) and (6) that

$$M_x + M_y = (1+\nu)M_{xv} = (1+\nu)M_{yv}\,. \tag{10}$$

With structures in reinforced concrete, where Poisson's ratio is usually equated to zero, this yields

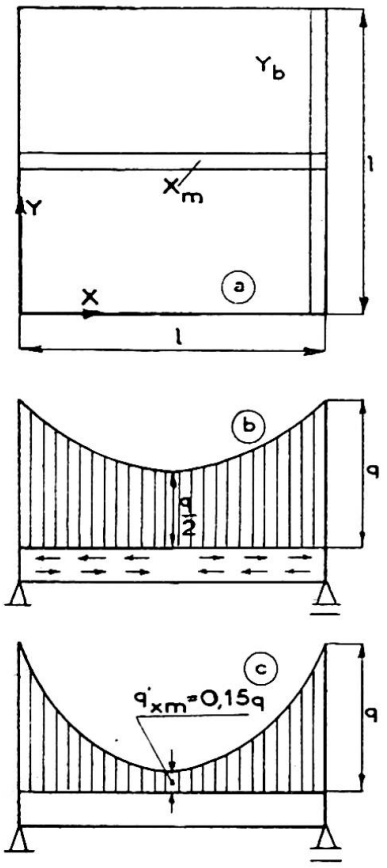

Fig. 2.

$$M_x + M_y = M_{xv} = M_{yv} \qquad (11)$$

or
$$M_x = M_{xv} - M_y \qquad (12)$$

and
$$M_y = M_{yv} - M_x \,. \qquad (13)$$

Furthermore it follows from eq. (4) and also by comparison of eqs. (1) and (12) that, with $\nu = 0$,

$$M_{x'} = -M_y \quad (14) \quad \text{and} \quad M_{y'} = -M_x \quad (15)$$

the latter equation following from the first one by changing x and y.

For example we shall use eq. (11) in order to find the bending moment in the centre of a square plate with sides l which carries a uniform load $q = \text{const.}$ (fig. 2 a). As at the edges $M_x = M_y = 0$ according to eq. (10) in any section of a boundary strip Y_b the moment M_{yv} will be zero too, so that for these strips q_y must be zero. Therefore, according to eq. (8), at $x = 0$ and $x = l$ the middlemost X-strip X_m has to carry a load $q_x = q$, whilst at $x = l/2$, on account of symmetry, $q_x = q_y = q/2$, so that q_x is distributed according to fig. 2b. Assuming a parabolic limitation of q_x we find that in the middle of X_m

$$M_{xv} = \frac{1}{8} q l^2 - \frac{5}{48} \frac{q}{2} l^2 = \frac{7}{96} q l^2$$

so that, because in the centre of the plate $M_x = M_y$, eq. (11) yields

$$M_x = M_y = \tfrac{1}{2} M_{xv} = \frac{7}{192} q l^2 = 0.0365\, q l^2 \,.$$

According to Nadai (5) the real bending moment with $\nu = 0$ is $0.0368\, q l^2$, so that our result is sufficiently accurate.

In order to find the equation of the deflection surface we remark that according to eq. (14) the moment $M_{x'}$ in X_m is distributed as $-M_y$, consequently practically as the negative deflection w_x of X_m, so that it may be

(5) Nadai, *Elastische Platten*, Berlin, 1925.

assumed to be caused by a fictituous load, being distributed according to the second differential quotient of w_x, consequently as $-M_x$. Assuming again a parabolic limitation of the total fictituous load q_x' according to fig. 2c, it follows that

$$M_{xm} = \frac{1}{8} q l^2 - \frac{5}{48} (q - q'_{xm}) l^2 = \frac{7}{192} q l^2$$

or $q'_{xm} = 0.15\, q$. The deflection w_x of X_m follows from q_x' by integrating four times and dividing by EI. Assuming the deflections of the other X-strips to be proportional to those of X_m, we obtain in this way the deflection surface of the square plate

$$w = \frac{8}{104\,175} \frac{q l^4}{E\mathcal{J}} (24\,\xi - 65\,\xi^3 + 75\,\xi^4 - 51\,\xi^5 + 17\,\xi^6) \cdot (24\,\eta - 65\,\eta^3 + 75\,\eta^4 - 51\,\eta^5 + 17\,\eta^6) \quad (16)$$

in which $\xi = x/l$ and $\eta = y/l$ and from which the bending and twisting moments at any point may be calculated immediately. These are situated fairly between the values obtained by Marcus ([2]) and Lewe ([6]), as was shown in our third paper in footnote 3. In a similar way we found for a square plate with a hydrostatic load $q = xp/l$ the deflection surface

$$w = \frac{8}{2\,187\,675} \frac{p l^4}{E\mathcal{J}} (208\,\xi - 217\,\xi^3 - 42\,\xi^5 + 51\,\xi^7) \cdot (24\,\eta - 65\,\eta^3 + 75\,\eta^4 - 51\,\eta^5 + 17\,\eta^6) \quad (17)$$

Various boundary conditions

If an X-strip is for example fixed at two sides (fig. 3), the moment $M_{x\tau} = -M_y$, that would be caused in it by the twisting stresses τ_{yx} if it were simply supported, being $-M_{ym}$ in the middle of the strip, will cause moments $\varphi_{xc} M_{ym}$ at the clamped edges (fig. 3b and 3c), by which at the crossing M of the most loaded strips X_m and Y_m we get, instead of eqs. (12) and (13)

$$M_{xm} = M_{xv} - \varphi_x M_{ym} \quad (18)$$

and

$$M_{ym} = M_{yv} - \varphi_y M_{xm}\,. \quad (19)$$

As for example along X_m the moment $M_{x\tau} = -M_y$ is about proportional to the deflection w_x of X_m, values φ_x or φ_y may be calculated if the ratios of the ordinates of w_x or w_y are known.

Also to this effect we remark that, by the twisting moments M_{xy} alone, the Y-strips, that cross X_m, would obtain deflections $w_{y\tau}$ according to curve 1 in fig. 3d, being proportional to $M_{y\tau} = -M_x$. As at their crossing with X_m their real deflections coincide with the deflection w_x of X_m, given by curve 2, the part q_y they take there of the total load q will be about proportional to $w_x - w_{y\tau}$, being the distance between curves 1 and 2. Assuming a uniformly distributed load q, we therefore find the

([6]) LEWE, *Pilzdecken*, Berlin, 1926.

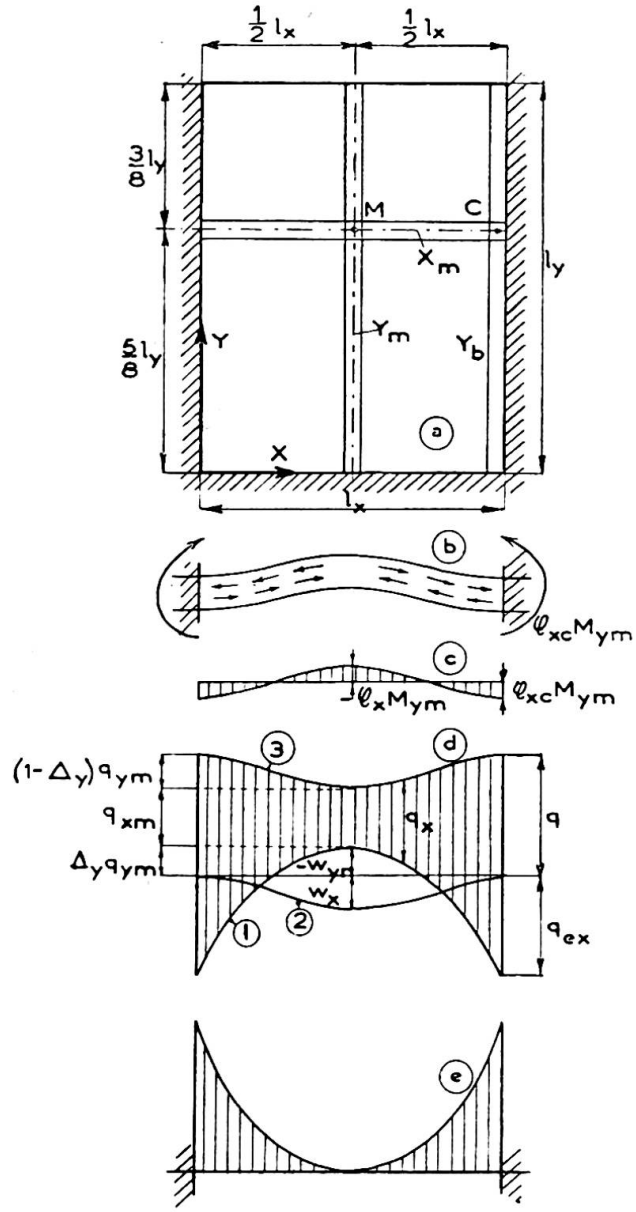

Fig. 3.

vertical load q_x on X_m by drawing curve 3 at a distance q above curve 2, load q_x being denoted by cross hatching. It follows that near a clamped edge the Y-strips cause an excess load q_{ex} on X_m instead of discharging it. Value q_{ex} was computed from the condition that the load q_y, taken by the boundary strip Y_b, being $q_y = -q_{ex}$ at C, has to cancel the bending moments

$$M_{y\tau} = -M_{xc}$$

caused by the twisting stresses τ_{yx}, in which M_{xc} is the moment M_x along the clamped edge. For a square plate with all edges built in q_{ex} is e.g. 0.61 q.

At the crossing M of the most loaded strips (fig. 3*a*)

$$q_{xm} + q_{ym} = q \tag{20}$$

whilst the deflections of X_m and Y_m in M must be equal. Expressing these deflections in the maximum positive moments M_{xm} and M_{ym} and assuming for that the same relations which hold for uniform load, this condition gives us the relation

$$M_{xm} = \mu\varepsilon^2 M_{ym} \tag{21}$$

in which $\varepsilon = l_y/l_x$, whilst for the six cases we considered (fig. 4, where a single line denotes a simply supported and cross hatching a clamped edge) μ is 1, 1, 1, 0.6, 32/45 and 27/32 respectively. Furthermore in fig. 3*d* the deflection $w_{y\tau}$ of Y_m is the result of the twisting moments M_{xy},

Fig. 4.

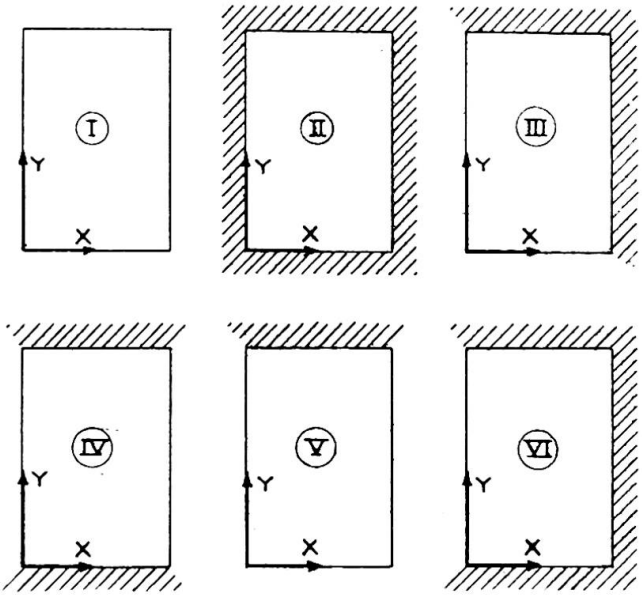

which cause in M a moment $-\varphi_y M_{xm}$ in Y_m. At the other hand w_x may be considered to be the result of the actual bending moment M_y in Y_m, being M_{ym} in M, so that, according to eq. (21) and fig. 3*d* we have e.g.

$$\Delta_y = \frac{-w_{yz}}{w_x - w_{yz}} = \frac{\varphi_y M_{xm}}{M_{ym} + \varphi_y M_{xm}} = \frac{\mu\varepsilon^2 \varphi_y}{1 + \mu\varepsilon^2 \varphi_y} \tag{22}$$

We could show ([3]) that for values ε between 0.5 and 2 it is sufficiently accurate to assume curve 1 in fig. 3*d*, the ordinates of which are proportional to $-M_x$, as a parabola, if M_{xm} and M_{ym} are considered as the maximum positive moments in the strips and not always as those in M. Then also curve 3, being proportional to w_x, may be easily found. For we showed above here that the effect of the twisting stresses on X_m is equivalent to that of a fictituous load proportional to $-M_x$, so that the deflection w_x is between that by a uniform and that by a parabolic load, the latter being indicated in fig. 3*e*. With known shapes of w_x and w_y values φ_x, φ_{xc}, φ_y and φ_{yc} can also be computed. The only unknown values in fig. 3*d* being now q_{xm} and q_{ym}, we may calculate

$$M_{xv} = m(q_{xm} + eq_{ym} + fq_{ex})\, l_x^2 \tag{23}$$

whilst in the same way we find

$$M_{yv} = n(q_{ym} + gq_{xm} + hq_{ey})\, l_y^2 . \tag{24}$$

Consequently we have six equations, (18), (19), (20), (21), (23) and (24), with six unknown values, q_{xm}, q_{ym}, M_{xv}, M_{yv}, M_{xm} and M_{ym}. In this way we got the maximum positive moments M_{xm} and M_{ym}, whence we obtain also the clamping moments

$$M_{xc} = M_{xvc} + \varphi_{xc} M_{ym} \tag{25}$$

and

$$M_{yc} = M_{yvc} + \varphi_{yc} M_{xm} . \tag{26}$$

For values $\varepsilon = l_y/l_x$ between 0.5 and 2 we got

$$\left.\begin{aligned} &M_{xm} = mq_x' l_x^2 \quad \text{and} \quad M_{ym} = nq_y' l_y^2 \\ \text{with} \quad &q_x' = \beta \frac{\varepsilon^4}{\varepsilon^4 + \gamma\varepsilon^2 + \alpha'} q , \qquad q_y' = \beta \frac{\alpha}{\varepsilon^4 + \gamma\varepsilon^2 + \alpha'} q \end{aligned}\right\} \tag{27}$$

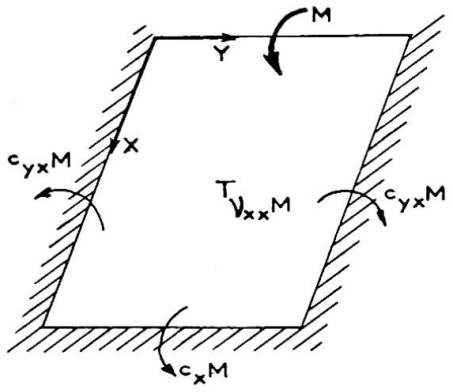

Fig. 5.

$$M_{xc} = m_c q_{xc}' l_x^2 \quad \text{and} \quad M_{yc} = n_c q_{yc}' l_y^2$$

$$\text{with} \quad q_{xc}' = \lambda_x \frac{\varepsilon^4 + \omega_x \varepsilon^2 + \rho_x}{\varepsilon^4 + \gamma \varepsilon^2 + \alpha'} q \leqslant q \,, \qquad q_{yc}' = \lambda_y \frac{1 + \omega_y \varepsilon^2 + \rho_y \varepsilon^4}{\varepsilon^4 + \gamma \varepsilon^2 + \alpha'} q \leqslant q \tag{28}$$

If we put q_{ex} and q_{ey} equal to their values for $\varepsilon = 1$, values β, γ, α', etc. are constants ([7]). Somewhat more accurate values could be obtained, however, by taking into accunt the variation of q_{ex} and q_{ey} with ε. In order to avoid that by this β, γ, α', etc. would become functions of ε, we expressed q_{ex} and q_{ey} in q_{xm} and q_{ym}, by which β, γ, α', etc. remained constant in the intervals $\varepsilon = 0.5 - 1$ and $\varepsilon = 1 - 2$ ([8]). In table I, where cases I_u - VI_u refer to the 6 cases in fig. 4 and to uniform load, all values of eqs (27) and (28) are given.

Only for the moments along the short clamped edges it is not allowed to assume curve 1 in fig. 3*d* as a parabola. These clamping moments we derived as follows. M_{yc} for case II_u we found by superimposing on the deflection of a square plate, with sides l_x, for which M_{yc} is known (see also under here), a deflection of one of the clamped edges according to that of the middle strip X_m in case $\varepsilon = 2$, yielding $M_{yc} = -0.057\, q l_x^2$. Subsequently we found M_{yc} for case IV_u and $\varepsilon = 2$ by remarking that here the X-strips, with lengths l_x, have the same rigidity as if they were clamped with lengths $l_x' = l_x \sqrt[4]{5}$, so that M_{yc} has about the same value as for case II_u and $\varepsilon = \frac{2}{\sqrt[4]{5}} = 1.34$, being

$$M_{yc} = -0.057\, q l_x'^2 = -0.127\, q l_x^2 \,.$$

As, however, here $q_{ey} = 1.22\, q$ instead of $1.32\, q$ for case II_u, we have to multiplicate this value with about 2.22/2.32, yielding $M_{yc} = -0.120\, q l_x^2$. Using the carry-over factors, mentioned under here, we computed from these values M_{xc} and M_{yc} *for* $\varepsilon = 0.5$ and 2 for the other cases (fig. 4). Demanding that $dM_c/d\varepsilon$ is continuous at $\varepsilon = 1$ and zero at $\varepsilon = 0.5$ and 2, we obtain for $\varepsilon < 1$ and $\varepsilon > 1$ respectively

$$M_{xc} = [-A + B(\varepsilon - 0.5)^p]\, q l_y^2 \quad \text{and} \quad M_{yc} = [-C + D(2 - \varepsilon)^p]\, q l_x^2 \tag{29}$$

([7]) Bijlaard, *De Ingenieur*, n° 23, 1935.
([8]) Bijlaard, *De Ingenieur in Ned. Indië*, n° 12, 1935.

in which A, B, C, D and p are given in table II. For case VI and $\varepsilon < 1$ we got

$$M_{xc} = [-0.057 - 0.06\,(\varepsilon - 0.5)^2 + 0.35\,(\varepsilon - 0.5)^5]\,ql_y^2 . \qquad (30)$$

In the same way we examined cases I and II (fig. 4) for hydrostatic load $q = xp/l_x$. As we considered both cases separately and disposed already of the data for uniform load, we could approximate the shapes of curves 1 and 3 (cf. fig. 3*d*), for which in case II we used curves of the fifth and seventh degree respectively, still better than before. Eqs. (27) and (28) hold here as well, the coefficients being given in table III (cases I_h and II_h), in which M_{xcu} and M_{xcl} refer to the upper ($x = 0$) and lower edge ($x = l_x$). For the clamping moments at the shorter edges we got for case II_h and $\varepsilon < 1$

$$M_{xcu} = 0.002\,(9 - 40\,\varepsilon + 22\,\varepsilon^2)\,pl_y^2 \quad \text{and} \quad M_{xcl} = 0.0066\,(4\,\varepsilon - 9)\,pl_y^2 \qquad (31)$$

whilst for $\varepsilon > 1$ the maximum clamping moment $M_{yc} = -0.028\,pl_x^2$. The better approximation appears from the fact, that with the values in table III it follows from case II_h and $\varepsilon = 1$ a clamping moment for uniform load $p = q$, being the sum of M_{xcu} and M_{xcl}, the value $M_{xc} = -0.0507\,ql_x^2$, whilst with our values for case II_u in table I we find directly $M_{xc} = -0.0529\,ql_x^2$, the accurate value being $M_{xc} = 0.0513\,ql_x^2$ ([9]). In the same way other cases may be examined. It is, however, easier to determine from our values for uniform load the carry-over factors c according to the Cross method of moment distribution (fig. 5). It is for example obvious that, with reference to the moments at the middles of the edges,

$$c_x = \frac{M_{xcVI} - M_{xcII}}{M_{xcII}} \quad \text{and} \quad c_{y.x} = \frac{1}{2}\,(1 - c_x)\,\frac{M_{ycIV} - M_{ycII}}{M_{xcII}} .$$

In a similar way we calculated the influence values ν of an edge moment M (fig. 5) for the positive moments in the slab. Furthermore we calculated the factors with which the clamping moments at the middle of the sides have to be multiplicated to get the maximum edge moments. We found for example the coefficients for case VI_h for hydrostatic load (edge $x = 0$ simply supported), as given in table III, by superimposing the influence of a moment, opposite to M_{xcu}, on the moments for case II_h. We have e.g. $M_{xclVI} = M_{xclII} + c_x M_{xcuII}$. The clamping moments at the shorter sides are

$$M_{xcl} = [-0.0352\,(2 - \varepsilon) + 0.072\,(1 - \varepsilon)^2 - 0.09\,(1 - \varepsilon)^3]\,pl_y^2$$

and

$$M_{yc} = [-0.0367 + 0.0074\,(2 - \varepsilon)^4]\,pl_x^2 . \qquad (32)$$

Moreover, using the carry-over factors c, we are able to calculate continuous floor slabs, starting from case II for all plates, according to the Cross method, whereby we can also allow for the torsional rigidities of the beams. After having found the final edge moments we correct the positive moments in the slabs by means of the partial influence values ψ of the edge moments, being valid if each edge moment varies separately.

These values ψ were calculated in another way by Bittner ([10]) (his values μ). From our data for uniform and hydrostatic load we determined

---

([9]) Timoshenko, *Theory of Plates and Shells*, 1940, p. 228.

([10]) Bittner, *Momententafeln und Einflussflächen für kreuzweise bewehrte Eisenbetonplatten*, Vienne, 1938.

Case	m	n	m_c	n_c	α	$\varepsilon = 1-2$						$\varepsilon = 0{,}5-1$					
						β	α'	γ	λ_x	ω_x	ρ_x	β	α'	γ	λ_y	ω_y	ρ_y
I_u	1/8	1/8	—	—	1	7/6	1	2	—	—	—	7/6	1	2	—	—	—
II_u	1/24	1/24	—1/12	—1/12	1	1.21	0.91	0.86	1.18	0.27	0.22	1.32	1.09	0.94	1.30	0.27	0.22
III_u	9/128	9/128	—1/8	—1/8	1	1.20	0.94	1.33	1.20	0.37	0.24	1.29	1.07	1.42	1.28	0.37	0.24
IV_u	1/8	1/24	—	—1/12	5	1.26	5.22	3.08	—	—	—	1.43	6.19	3.34	6.88	0.22	0.07
V_u	1/8	9/128	—	—1/8	2.5	1.22	2.53	2.64	—	—	—	1.26	2.69	2.72	3.11	0.32	0.12
VI_u	9/128	1/24	—1/8	—1/12	2	1.23	1.94	1.55	1.23	0.40	0.38	1.36	2.29	1.68	2.66	0.25	0.14

TABLE I

Case	A	B	C	D	p
II_u	0.057	0.25	0.057	$0.004/\varepsilon^6$	6
III_u	0.08	0.19	0.08	$0.006/\varepsilon^5$	5
IV_u	—	—	0.12	0.05	2
V_u	—	—	0.12	0.033	3
VI_u	—	—	0.08	0.018	4

TABLE II

Case	m	n	m_c	n_c	$\varepsilon = 1-2$									
					β	$\beta\alpha$	α'	γ	λ_{xu}	ω_{xu}	ρ_{xu}	λ_{xl}	ω_{xl}	ρ_{xl}
I_h	1/8	1/8	—	—	0.62	0.52	0.78	1.76	—	—	—	—	—	—
II_h	1/24	1/24	--1/12	--1/12	0.62	0.58	0.84	0.82	0.50	0.15	0.01	0.71	0.25	0.21
VI_h	9/128	1/24	--1/8	--1/12	0.47	0.94	1.92	0.80	—	—	—	0.64	0.04	0.60

Case	$\varepsilon = 0.5-1$							
	β	$\beta\alpha$	α'	γ	λ_y	ω_y	ρ_y	
I_h	$0.62\,\Phi_1$	0.52	0.78	1.76	—	—	—	$\Phi_1 = 2\varepsilon^2 - 4\varepsilon + 3$
II_h	$0{,}67\,\Phi_1$	$0.126\,\Phi_2$	0.97	0.88	$0.124\,\Phi_2$	0.28	0.23	$\Phi_2 = 2\varepsilon^2 - 4\varepsilon + 7$
VI_h	$0.09\,\Phi_3$	$0.18\,\Phi_2$	1.42	1.14	$0.175\,\Phi_2$	0.31	0.12	$\Phi_3 = 18\varepsilon^2 - 36\varepsilon + 23$

TABLE III

$-M_{yc}$	Timoshenko			Bijlaard			Multiplier
Case	II_u	IV_u	V_u	II_u	IV_u	V_u	
$\varepsilon = 0.5$	0.083	0.084	0.122	0.083	0.083	0.123	ql_y^2
$\varepsilon = 1$	0.051	0.070	0.084	0.053	0.070	0.087	ql_y^2
$\varepsilon = 2$	0.057	0.119	0.122	0.057	0.120	0.120	ql_x^2

TABLE IV

values ω and φ according to Bittner too for values $\varepsilon = 0.5 - 2$. It is evident that for uniform load e.g. $\omega_y = -M_{ycV}$ and that $\varphi_y = \frac{M_{ycV} - M_{ycIV}}{M_{ycIV}}$, so that, in cases where this is easier, we can calculate a slab in this way too (11).

In table IV we compared the clamping moments M_{yc} according to our formulae with those according to Timoshenko (12) for cases II_u, IV_u and V_u and $\varepsilon = 0.5$, 1 and 2.

Résumé

Par une méthode approximative nous obtenons des formules simples et générales nous permettant de déterminer, avec une approximation suffisante, les moments fléchissants maxima positifs et négatifs. Ces moments ainsi déterminés, nous pouvons calculer les coefficients de transmission utilisés pour le calcul des dalles continues selon la méthode de Cross.

Zusammenfassung

Durch ein Näherungsverfahren werden für die grössten positiven und negativen Biegungsmomente einfache allgemeine Formeln von genügender Genauigkeit erhalten. Mit den so berechneten Werten können die Uebertragungskoeffizienten bestimmt werden, die es erlauben, durchlaufende Platten auch nach dem Momentenverteilungsverfahren von Cross zu berechnen.

Summary

By an approximative method simple general formulae have been obtained for the maximum positive and negative bending moments, which give more than sufficiently accurate results. From the data obtained in this way the carry-over factors were calculated, by which the bending moments in continuous floors may also be computed by the Cross method of moment distribution.

(11) These values ω_y and φ_y have nothing to do with *our* values ω_y, φ_y, etc.

(12) TIMOSHENKO, *Theory of Plates and Shells*, 1940, pp. 228, 206 and 213 resp.

Leere Seite
Blank page
Page vide

IVb2

Flexion et flambage d'un certain type de plaques continues orthotropes

Biegung und Beulung eines bestimmten Types von durchlaufenden orthotropen Platten

Bending and buckling of some types of continuous orthotropic plates

PROF. Dr W. NOWACKI
Gdansk

Flexion des plaques continues

I. L'équation différentielle connue de flexion d'une plaque orthotrope ([1]) est posée comme suit

$$D_x \frac{\partial^4 w}{\partial x^4} + 2H \frac{\partial^4 w}{\partial x^2 \partial y^2} + D_y \frac{\partial^4 w}{\partial y^4} = p \qquad (1)$$

$$D_x = \frac{m_x m_y}{m_x m_y - 1} E_x \frac{h^3}{12} \qquad D_y = \frac{m_x m_y}{m_x m_y - 1} E_y \frac{h^3}{12} \qquad C = G_0 \frac{h^3}{12}$$

$$2H = \frac{D_x}{m_y} + \frac{D_y}{m_x} + 4C \qquad m_x E_x = m_y E_y$$

où E_x, E_y sont les modules d'élasticité suivant les axes x et y ;
m_x, m_y sont les nombres de Poisson pour ces directions ;
G_0 est la constante des matériaux (le corrélatif du module d'élasticité transversale pour plaque isotrope).

Les forces de section sont unies à la flexion dans (x, y) au moyen des relations suivantes (fig. 1) :

([1]) M. T. Huber : 1. *La théorie générale des hourdis en béton armé* (*Czasopismo techniczne*, Lwów, 1914); 2. *Teoria plyt.* (*Tow. Naukowe*, Lwów, 1921); 3. *Probleme der Statik technisch wichtiger orthotropen Platten*, Warszawa, 1929.

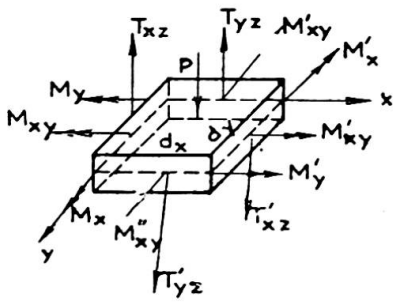

Fig. 1.

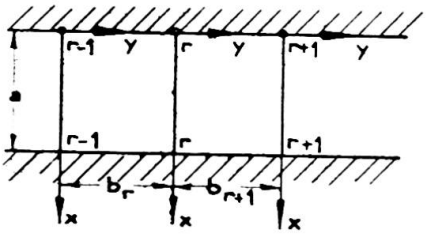

Fig. 2.

$$M_x = -D_x\left(\frac{\partial^2 w}{\partial x^2} + \frac{1}{m_y}\frac{\partial^2 w}{\partial y^2}\right) \qquad M_y = -D_y\left(\frac{\partial^2 w}{\partial y^2} + \frac{1}{m_x}\frac{\partial^2 w}{\partial x^2}\right)$$

$$M_{xy} = -2C\frac{\partial^2 w}{\partial x \partial y}$$

$$T_{xz} = -D_x\frac{\partial^3 w}{\partial x^3} + \left(\frac{D_x}{m_y} + 2C\right)\frac{\partial^3 w}{\partial x \partial y^2} \tag{2}$$

$$T_{yz} = -D_y\frac{\partial^3 w}{\partial y^3} + \left(\frac{D_y}{m_x} + 2C\right)\frac{\partial^3 w}{\partial y \partial x^2}$$

Dans le cas de plaque isotrope

$$D_x = D_y = D \qquad m_x = m_y = m \qquad C = \frac{1}{2}\frac{m-1}{m}D.$$

II. Considérons l'élément de la plaque continue, limité par les droites $x=0$, $x=a$, ainsi que par les droites $y=0$, $y=b$ (fig. 2). Sur les droites d'appui $y=0$, $y=b$, $x=0$, $x=a$ se produiront les moments fléchissants et de torsion. Les moments fléchissants $M_y(x, 0)$ sur les lignes d'appui $y=0$, $y=b$, ainsi que les moments $M_x(0, y)$ sur les lignes d'appui $x=0$, $x=a$ seront considérés comme grandeurs hyperstatiques.

Pour déterminer les moments $M_y(x, 0)$ et $M_x(0, y)$ nous allons profiter des conditions de continuité de la plaque sur ces appuis.

Cependant, avant de poser les équations conditionnelles on doit étudier le système fondamental de la plaque à appui libre le long de ses bords, uniformément chargée du poids p ainsi que par le moment

$$M_y(x, 0) = \sum_n^{\infty} Kn \sin\frac{n\pi x}{a}$$

le long de l'arête $y=0$.

a) *Charge de la plaque par le moment* $\sum_{1,2}^{\infty} Kn \sin\frac{n\pi x}{a}$ (fig. 3).

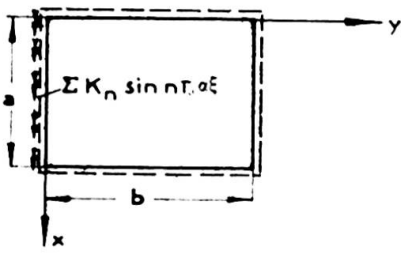

Pour ce genre de charge aux données

$$y = \eta b \qquad x = \xi b \qquad b = \alpha a$$

$$\varepsilon^4 = \frac{D_x}{D_y} \qquad \rho = \frac{H}{\sqrt{D_x D_y}}$$

Fig. 3.

nous amenons l'équation (1) à l'expression sans dimension

$$\frac{\partial^4 w}{\partial \eta_1^4} + 2\rho\varepsilon^2 \frac{\partial^4 w}{\partial \xi^2 \partial \eta_1^2} + \varepsilon^4 \frac{\partial^4 w}{\partial \xi^4} = 0 . \tag{3}$$

Admettant que

$$w = \sum_{n=1,2}^{\infty} Y_n(\eta_1) \sin n\pi\alpha\xi$$

nous transformons l'équation (3) en

$$Y_n^{(IV)} - 2\rho\nu^2 Y_n'' + \nu^4 Y_n = 0 \qquad \nu = \varepsilon n\pi\alpha \tag{4}$$

L'équation caractéristique

$$r^4 - 2\rho\nu^2 r^2 + \nu^4 = 0$$

donne quatre racines.

I $\quad \rho > 1 \quad r_{1,2} = \pm\lambda_1 \quad r_{3,4} = \pm\lambda_2 \quad \lambda_{1,2} = \nu\sqrt{\rho \pm \sqrt{\rho^2 - 1}}$

II $\quad \rho = 1 \quad r_{1,2} = \nu \quad r_{3,4} = -\nu$

III $\quad \rho < 1 \quad r_{1,2} = \varphi_1 \pm i\varphi_2 \quad r_{3,4} = -(\varphi_1 \pm i\varphi_2) \quad \varphi_{1,2} = \nu\sqrt{\frac{1 \pm \rho}{2}}$

où $$\lambda_{1,2} = \varphi_1 \pm i\varphi_2 .$$

Nous allons considérer le premier cas uniquement; nous obtiendrons l'intégrale du deuxième cas au moyen de passage aux limites; le passage du premier cas au troisième s'effectuera par voie de substitution

$$\lambda_{1,2} = \varphi_1 \pm i\varphi_2 .$$

Pour $\rho > 1$ la solution générale de l'équation (4) sera

$$Y_n(\eta_1) = U_{1n}\cos\lambda_1\eta_1 + U_{2n}\sin\lambda_1\eta_1 + U_{3n}\cos\lambda_2\eta_1 + U_{4n}\sin\lambda_2\eta_1 . \tag{5}$$

Les constantes d'intégration $U_{1n}, \ldots, U_{4n}$ seront déterminées par les conditions des bords de la plaque

$$Y_n(0) = 0 \qquad Y_n(1) = 0 \qquad Y''(0) = -\frac{Kn\, b^2}{D_y} \qquad Y''(1) = 0 .$$

Nous trouverons

$$U_{1n} = -\frac{K_n b^2}{2 D_y \nu^2} \cdot \frac{1}{\sqrt{\rho^2 - 1}} ; \qquad U_{2n} = -U_{1n}\operatorname{ctg}\lambda_1$$

$$U_{3n} = -U_{1n} \qquad U_{4n} = U_{1n}\operatorname{ctg}\lambda_2 . \tag{6}$$

L'inclinaison de la surface de flexion de la plaque le long de l'arête $y = 0$ et de $y = b$ donne

$$\left.\frac{\partial w}{\partial y}\right|_{y=0} = \frac{b}{D_y}\sum_{n=1,2}^{\infty} K_n \Phi_n \sin n\pi\alpha\xi \qquad \left.\frac{\partial w}{\partial y}\right|_{y=b} = -\frac{b}{D_y}\sum_{n=1,2}^{\infty} K_n \Psi_n \sin n\pi\alpha\xi \tag{7}$$

$$\Phi_n = \frac{1}{2\nu^2\sqrt{\rho^2 - 1}} \cdot \frac{\lambda_1 \cos\lambda_1 \sin\lambda_2 - \lambda^2 \cos\lambda_2 \sin\lambda_1}{\sin\lambda_1 \sin\lambda_2} \tag{8}$$

$$\Psi_n = \frac{1}{2\nu^2\sqrt{\rho^2-1}} \cdot \frac{\lambda_2 \sin\lambda_1 - \lambda_1 \sin\lambda_2}{\sin\lambda_1 \sin\lambda_2} \tag{9}$$

L'angle d'inclinaison de la surface de flexion aux arêtes $x=0$, $x=a$

$$\left.\frac{\partial w}{\partial x}\right|_{x=0} = \frac{\pi}{a}\sum_{n=1,2}^{\infty} n Y_n(\eta) \qquad \left.\frac{\partial w}{\partial x}\right|_{x=a} = \frac{\pi}{a}\sum_{n=1,2}^{\infty} n(-1)^n Y_n(\eta) \tag{10}$$

sera transformé par le développement de la fonction $Y_n(\eta)$ en série de Fourier, en série double infinie

$$\left.\frac{\partial w}{\partial x}\right|_{x=0} = \frac{a}{D_x}\sum_{n}^{\infty}\sum_{i}^{\infty} K_n A_{i,n} \sin i\pi\eta$$

$$\left.\frac{\partial w}{\partial x}\right|_{x=a} = \frac{a}{D_x}\sum_{n}^{\infty}\sum_{i}^{\infty} K_n A_{i,n} (-1)^n \sin i\pi\eta$$

où

$$A_{i,n} = \frac{i}{n^3\pi^2\alpha^2} \cdot \frac{1}{\left[1 + 2\rho\left(\frac{i}{n\alpha\varepsilon}\right)^2 + \left(\frac{i}{n\alpha\varepsilon}\right)^4\right]} \quad \rho \gtreqless 1. \tag{11}$$

b) *Charge par le moment* $M = \sum_{n}^{\infty} K_n \sin n\pi\alpha\xi$ *le long de l'arête* $y = b$ (fig. 4).

Sans changer les constantes d'intégration $U_{1n}, \ldots, U_{4n}$ (équation 6) il faut dans la fonction $Y_n(\eta)$ (équation 5) poser $\eta' = 1 - \eta$ au lieu de η.

En conséquence

$$\left.\frac{\partial w}{\partial y}\right|_{y=0} = \frac{b}{D_y}\sum_{n}^{\infty} K_n \Psi_n \sin n\pi\alpha\xi \qquad \left.\frac{\partial w}{\partial y}\right|_{y=b} = -\frac{b}{D_y}\sum_{n}^{\infty} K_n \Phi_n \sin n\pi\alpha\xi$$

$$\left.\frac{\partial w}{\partial x}\right|_{x=0} = -\frac{a}{D_x}\sum_{n}^{\infty}\sum_{i}^{\infty} K_n (-1)^i A_{i,n} \sin i\pi\eta$$

$$\left.\frac{\partial w}{\partial x}\right|_{x=a} = -\frac{a}{D_x}\sum_{n}^{\infty}\sum_{i}^{\infty} K_n (-1)^{i+n} A_{i,n} \sin i\pi\eta\,.$$

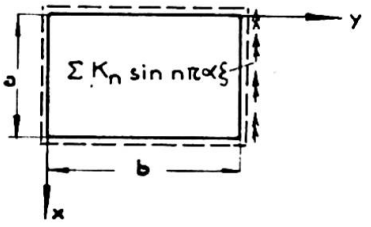

Fig. 4.

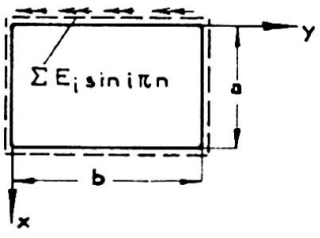

Fig. 5.

c) *Le moment* $M=\sum_{i}^{\infty} E_i \sin i\pi\eta$ *agit le long de l'appui* $x=0$ (fig. 5).

Admettant que $w=\sum_{n}^{\infty} \chi_i \sin i\pi\eta$

nous amenons l'équation (3) à l'expression

$$X_i^{IV} - 2\rho\theta^2 X_i'' + \theta^4 X_i = 0 \qquad \theta = \frac{i\pi}{\varepsilon} .$$

Pour $\rho > 1$ nous obtiendrons la solution générale

$$X_i(\xi) = U_{1i}\cos\mu_1\xi + U_{2i}\sin\mu_1\xi + U_{3i}\cos\mu_2\xi + U_{4i}\sin\mu_2\xi \qquad (12)$$

$$\mu_{1.2} = \theta\sqrt{\rho \pm \sqrt{\rho^2 - 1}} .$$

Des conditions des bords

$$X_i(\theta) = 0 \qquad X_i\left(\frac{1}{\alpha}\right) = 0 \qquad X_i''(\theta) = -\frac{E_i a^2}{D_x} \qquad X_i''\left(\frac{1}{\alpha}\right) = 0$$

nous obtiendrons

$$U_{1i} = -\frac{E_i a^2}{2 D_x \omega^2}\cdot\frac{1}{\sqrt{\rho^2 - 1}} \quad U_{2i} = U_{1i}\operatorname{ctg}\chi_1 \quad U_{3i} = -U_{1i}$$
$$U_{4i} = U_{1i}\operatorname{ctg}\chi_2 \qquad (13)$$
$$\omega = \frac{\theta}{\alpha} \qquad \chi_{1,2} = \frac{\mu_{1,2}}{\alpha} .$$

Ensuite

$$\left.\frac{\partial w}{\partial x}\right|_{x=0} = \frac{a}{D_x}\sum_{i}^{\infty} E_i \Phi_i \sin i\pi\eta \qquad \left.\frac{\partial w}{\partial x}\right|_{x=a} = -\frac{a}{D_x}\sum_{i}^{\infty} E_i \Psi_i \sin i\pi\eta$$

où

$$\Phi_i = \frac{1}{2\omega^2\sqrt{\rho^2 - 1}}\cdot\frac{\chi_1\cos\xi_1\sin\chi_2 - \chi_2\cos\chi_2\sin\chi_1}{\sin\chi_1\sin\chi_2} ;$$
$$\Psi_i = \frac{1}{2\omega^2\sqrt{\rho^2 - 1}}\cdot\frac{\chi_2\sin\chi_1 - \chi_1\sin\chi_2}{\sin\chi_1\sin\chi_2} \qquad (14)$$

Et enfin

$$\left.\frac{\partial w}{\partial y}\right|_{y=0} = \frac{b}{D_y}\sum_{i}^{\infty}\sum_{n}^{\infty} E_i B_{i,n}\sin i\pi\alpha\xi$$

$$\left.\frac{\partial w}{\partial y}\right|_{y=b} = \frac{b}{D_y}\sum_{i}^{\infty}\sum_{n}^{\infty} E_i B_{i,n}(-1)^i\sin i\pi\alpha\xi$$

où

$$B_{i,n} = \frac{n\alpha^2}{\pi^2 i^3\left|1 + 2\rho\left(\frac{n\alpha\varepsilon}{i}\right)^2 + \left(\frac{n\alpha\varepsilon}{i}\right)^4\right|} \quad \rho \gtrless 1 . \qquad (15)$$

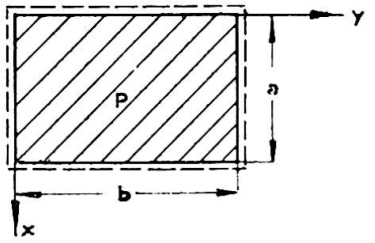

Fig. 6.

d) *Charge de la plaque par* p = const. (fig. 6).

La surface de flexion est traduite par l'équation

$$w=\frac{4\,pa^4}{D_x}\sum_{n=1,3}^{\infty}\left[\left(\frac{1}{n\pi}\right)^5+Y_n(\eta_1)\right]\sin n\pi\alpha\xi \qquad \overline{Y}_n=\left(\frac{1}{n\pi}\right)^5+Y_n(\eta_1). \tag{16}$$

Ici la fonction $Y_n(\eta)$ est identique à la fonction $Y_n(\eta_1)$ de l'équation (5).

Nous déterminons les constantes d'intégration des conditions aux limites suivantes

$$\overline{Y}_n(0)=0\,, \quad \overline{Y}_n''(0)=0\,, \quad \overline{Y}_n(1)=0\,, \quad \overline{Y}_n''(1)=0\,.$$

D'où pour $\rho>1$

$$U_{1n}=\left(\frac{1}{n\pi}\right)^5\frac{\lambda_2^2}{2\nu^2\sqrt{\rho^2-1}}\,; \qquad U_{2n}=U_{1n}\frac{1-\cos\lambda_1}{\sin\lambda_1}$$

$$U_{3n}=-U_{1n}\frac{\lambda_1^2}{\lambda_2^2}\,; \qquad U_{4n}=\frac{\lambda_1^2}{\lambda_2^2}\frac{\cos\lambda_2-1}{\sin\lambda_2}U_{1n}. \tag{17}$$

L'inclinaison de la plaque aux arêtes $y=0$ et $y=b$ sera amenée à l'expression

$$\left.\frac{\partial w}{\partial y}\right|_{y=0}=-\left.\frac{\partial w}{\partial y}\right|_{y=b}=\frac{4\,pb^3}{D_y}\sum_{n=1,3}^{\infty}\Theta_n\sin n\pi\alpha\xi$$

$$\Theta_n=\frac{\varepsilon\alpha^2}{2\nu^5\sqrt{\rho^2-1}}\left[\lambda_1\frac{\cos\lambda_2-1}{\sin\lambda_2}-\lambda_2\frac{\cos\lambda_1-1}{\sin\lambda_1}\right]. \tag{18}$$

Dans la suite de nos considérations nous allons profiter du développement de la surface de flexion de la plaque en série

$$w=\frac{4\,pb^4}{D_y}\sum_{i=1,3}^{\infty}\left[\left(\frac{1}{i\pi}\right)^5+X_i(\xi)\right]\sin i\pi\eta_1\,. \tag{19}$$

L'inclinaison de la plaque aux arêtes $x=0$ ainsi que $x=a$ donne pour $\rho>1$

$$\left.\frac{\partial w}{\partial x}\right|_{x=0}=-\left.\frac{\partial w}{\partial x}\right|_{x=a}=\frac{4\,pa^3}{D_x}\sum_{i=1,3}^{\infty}\Theta_i\sin i\pi\eta_1$$

où

$$\Theta_i=\frac{1}{2\,\varepsilon\alpha\sqrt{\rho^2-1}\;\omega^5}\left[\chi_1\frac{\cos\chi_2-1}{\sin\chi_2}-\chi_2\frac{\cos\chi_1-1}{\sin\chi_1}\right] \tag{20}$$

et les constantes d'intégration

$$U_{1i}=\left(\frac{1}{i\pi}\right)^5 \frac{\chi_2^2}{2\,\omega^2\sqrt{\rho^2-1}}\;; \qquad U_{2i}=U_{1i}\frac{1-\cos\chi_1}{\sin\chi_1}\;;$$

$$U_{3i}=-\,U_{1i}\frac{\chi_1^2}{\chi_2^2} \qquad U_{4i}=U_{1i}\frac{\chi_1^2}{\chi_2^2}\,\frac{\cos\chi_2-1}{\sin\chi_2} \tag{21}$$

III. Considérons les deux aires contiguës de la plaque continue; l'aire r à la caractéristique d'orthotropie ρ_r et chargée de p_r, ainsi que l'aire $r+1$ à la caractéristique d'orthotropie ρ_{r+1} et chargée de p_{r+1}.

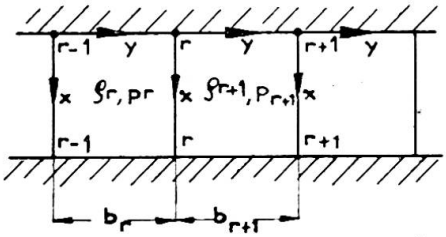

Fig. 7.

Nous nous bornerons à une plaque continue aux arêtes $x=0$, $x=a$ rigidement encastrée.

Désignons par M^{r-1}, M^r, M^{r+1} les moments d'appui M_y en droites $r-1$, r, $r+1$, en outre $M^r=\sum_n^{\infty} K_n^r \sin n\pi\alpha\xi$ et par M^r, M^{r+1} les moments M_x aux arêtes $x=0$, $x=a$ de l'aire r ainsi que de l'aire $r+1$; avec cela

$$M^r=\sum_i^{\infty} E_i^r \sin i\pi\eta.$$

La condition d'encastrement rigide de la plaque à l'arête $x=a$ ou bien $x=0$ de l'aire r de la plaque donne

$$\sum \frac{\partial w^{r+1}}{\partial x}\Big|_{x=0}=0$$

d'où

$$\frac{i}{\pi^2\alpha_{r+1}^2}\sum_n^{\infty}\frac{K_n^r-K_n^{r+1}(-1)^i}{n^3\left[1+2\rho\left(\frac{i}{n\alpha\varepsilon}\right)^2+\left(\frac{i}{n\alpha\varepsilon}\right)^4\right]_{r+1}}$$

$$+E_i^{r+1}(\Phi_i^{r+1}+\Psi_i^{r+1})+4\,p_{r+1}a^2\Theta_i^{r+1}=0 \tag{22}$$

$$(i=1,\,2,\,\ldots)\,, \qquad (n=1,\,3,\,5,\,\ldots)\,.$$

La condition de continuité de la plaque sur l'appui r-r conduit à l'équation

$$-\frac{\partial w^r}{\partial y}\Big|_{y=br}+\frac{\partial w^{r+1}}{\partial y}\Big|_{y=0}=0$$

ou bien à

$$\frac{n}{\pi^2}\left\{\beta^{r+1}\alpha^2{}_{r+1}\sum_i^{\infty}\frac{2\,E_i^{r+1}}{i^3\left[1+2\varrho\left(\frac{n\alpha\varepsilon}{i}\right)^2+\left(\frac{n\alpha\varepsilon}{i}\right)^4\right]_{r+1}}\right.$$

$$\left.-\beta^r\alpha_r{}^2\sum_i^{\infty}\frac{2\,E_i^r(-1)^i}{i^3\left[1+2\varrho\left(\frac{n\alpha\varepsilon}{i}\right)^2+\left(\frac{n\alpha\varepsilon}{i}\right)^4\right]_r}\right\}$$

$$+K_n^{r-1}\beta^r\Psi_n^r+K_n^r(\beta^r\Phi_n^r+\beta^{r+1}\Phi_n^{r+1})+K_n^{r+1}\Psi_n^{r+1}\beta^{r+1}$$

$$+4\,(p_r b_r{}^2\beta^r\Theta_n^r+p_{r+1}b^2{}_{r+1}\beta^{r+1}\Theta_n^{r+1})=0 \qquad (23)$$

$$(n=1,\ 3,\ 5,\ \ldots),\qquad (i=1,\ 2,\ \ldots)\,.$$

$\beta^r=\dfrac{D_y^0\,,\ b_r}{D_y^r\,b_0}$ où b_0 est la longueur comparative de la travée, et D_y^0 la caractéristique comparative de flexion de la plaque.

Dans le cas d'encastrement rigide de la plaque continue en droite $x=0$ et d'appui libre en droite $x=a$, il faut dans l'équation (22) poser $\Psi_i^{r+1}=0$ et dans l'équation (23) au lieu de $2E_i^{r+1}$, $2E_i^r$ la valeur seule E_i^{r+1}, E_i^r.

Les grandeurs i, n prennent les valeurs successives 1, 2, 3, ...

Enfin dans le cas de plaque continue librement appuyée le long des arêtes $x=a$, $x=0$ l'équation (22) n'est pas applicable et dans l'équation (23) il y a lieu de poser $E_i=0$. Nous obtiendrons de la sorte un système simple d'équations

$$K_n^{r-1}\beta^r\Psi_n^r+K_n^r(\beta^r\Phi_n^r+\beta^{r+1}\Phi_n^{r+1})$$

$$+K_n^{r+1}\beta^{r+1}\Psi_n^{r+1}+4\,(p_r b_r{}^2\beta^r\Theta_n^r+p_{r+1}b^2{}_{r+1}\beta^{r+1}\Theta_n^{r+1})=0 \qquad (24)$$

$$(n=1,\ 3,\ 5,\ \ldots)\,.$$

Pour une plaque rigidement encastrée le long des quatre arêtes (aire $r+1$) $K_n^r=K_n^{r+1}=K_n$, $\beta^r=0$ et dans le cas particulier de plaque carrée $a=b$, $\alpha=1$, de même $K_n=E_n$.

Il en résulte le système d'équations

$$\frac{2n}{\pi^2}\sum_i^{\infty}\frac{E_i}{i^3\left[1+2\varrho\left(\frac{n\alpha\varepsilon}{i}\right)^2+\left(\frac{n\alpha\varepsilon}{i}\right)^4\right]}+E_n(\Phi_n+\Psi_n)+4\,pa^2\Theta_n=0$$

$$(n=1,\ 3,\ 5,\ \ldots)\,,\qquad (i=1,\ 3,\ 5,\ \ldots)\,.$$

Enfin pour plaque continue à libre appui le long des droites $x=0$, $x=a$, nous obtiendrons aux mêmes indices géométriques et d'élasticité ainsi qu'à la même charge $p=\text{const.}$ des aires, l'équation

$$K_n^{r-1}+2\,c_nK_n^r+K_n^{r+1}=W_n\,,\qquad c_n=\Phi_n/\Psi_n$$

$$(r=1,\ 2,\ \ldots,\ z-1)$$

$$W_n=\frac{8\,pb^2\,\Theta_n}{\Psi_n}$$

que nous pouvons considérer comme équation aux différences non homogène du second ordre. Et voici la solution de cette équation

$$K_n^r = -\frac{W_n}{2(1+c_n)}\left\{(-1)^r\left[\operatorname{tg}\frac{\omega z}{2}\sin\omega_r - \cos\omega_r\right] + 1\right\}$$

$$\omega = \ln\frac{1}{\sigma} \qquad \sigma = -c_n + \sqrt{c_n^2 - 1}$$

pour

$$z \to \infty \qquad K_n^r \approx -\frac{W_n}{2(1+c_n)} = -\frac{4\,pb^2\,\Theta_n}{\Psi_n + \Phi_n}\,.$$

Nous remarquons que dans chaque cas particulier le nombre d'équations est conforme au nombre d'inconnues. Les grandeurs K, E étant connues nous pourrons déterminer la surface de flexion de la plaque, et par conséquent les valeurs des forces de section des équations (2).

Flambage d'une plaque continue orthotrope à appui libre sur les arêtes

$$x = 0\,, \qquad x = a\,.$$

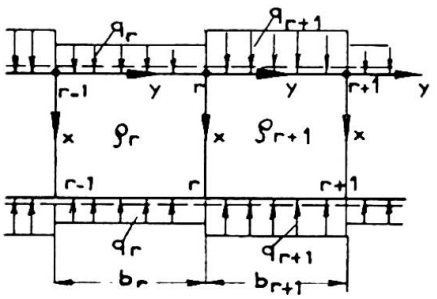

Fig. 8.

I. Pour $q > q_k$ (q_k = charge critique) la plaque fléchira et le long de l'arête $y = 0$ se produiront les moments fléchissants et de torsion.

L'équation différentielle du problème

$$D_x\frac{\partial^4 w}{\partial x^2} + 2H\frac{\partial^4 w}{\partial x^2\partial y^2} + D_y\frac{\partial^4 w}{\partial y^4} + q\frac{\partial^2 w}{\partial x^2} = 0 \qquad (25)$$

à l'aide des valeurs comme dans l'alinéa I*a* sera amenée à l'expression

$$\frac{\partial^4 w}{\partial\eta^4} + 2\rho\varepsilon^2\frac{\partial^4 w}{\partial\eta^2\partial\xi^2} + \varepsilon^4\frac{\partial^4 w}{\partial\xi^4} + \varepsilon^4\pi^2\varphi\frac{\partial^2 w}{\partial\xi^2} = 0 \qquad \varphi = \frac{qb^2}{\pi^2 D_x} \quad (25\,a)$$

Examinons tout d'abord le flambage d'une plaque rectangulaire librement appuyée sur trois arêtes et le long de la quatrième encastrée d'une façon élastique (fig. 9).

Admettant que

$$w = \sum_n^{\infty} Y_n(\eta)\sin n\pi\alpha\xi$$

nous obtiendrons

$$Y_n^{IV} - 2\rho\nu^2 Y_n'' + \nu^2(\nu^2 - \pi^2\varphi\varepsilon^2)\,Y_n = 0\,. \qquad (26)$$

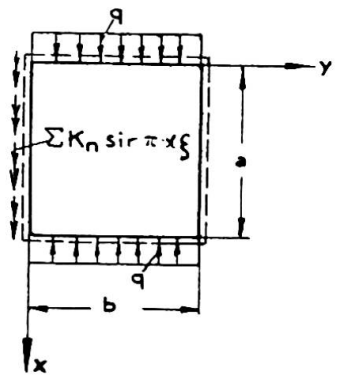

Fig. 9.

L'équation caractéristique

$$r^4 - 2\rho\nu^2 r^2 + \nu^2(\nu^2 - \pi^2\varphi\varepsilon^2) = 0$$

donne quatre racines.

Pour $\rho \gtreqless 1$ nous obtiendrons deux racines réelles et deux imaginaires

$$r_{1,2} = \pm m_1 \quad r_{3,4} = \pm i m_2 \quad m_{1,2} = \nu \sqrt{\sqrt{\rho^2 - 1 + \delta} \pm \rho}$$

$$\delta = \left(\frac{\pi\varepsilon}{\nu}\right)^2 \varphi \quad \nu = n\pi\alpha\varepsilon \,.$$

La solution générale de l'équation (26) sera la suivante

$$Y_n(\eta) = U_{1n} \cos m_1\eta + U_{2n} \sin m_1\eta + U_{3n} \cos m_2\eta + U_{4n} \sin m_2\eta \qquad (27)$$

$$m_1^2 + m_2^2 = 2\nu^2 \sqrt{\rho^2 - 1 + \delta} \qquad m_1^2 - m_2^2 = 2\nu^2\rho \,. \qquad (27a)$$

Les conditions aux limites du problème

$$Y_n(0) = 0 \qquad Y_n(1) = 0 \qquad Y_n''(0) = -\frac{K_n b^2}{D_y} \qquad Y_n''(1) = 0$$

conduisent aux constantes d'intégration

$$U_{1n} = -\frac{K_n b^2}{D_y} \frac{1}{m_1^2 + m_2^2} \qquad U_{3n} = -U_{1n}$$
$$U_{2n} = -U_{1n} \operatorname{ctg} m_1 \qquad U_{4n} = U_{1n} \operatorname{ctg} m_2 \,.$$

Les équations suivantes déterminent l'inclinaison de la surface de flexion aux arêtes $y = 0$, $y = b$

$$\left.\frac{\partial w}{\partial y}\right|_{y=0} = \frac{b}{D_y} \sum_n^\infty K_n \overline{\Phi_n} \sin n\pi\alpha\xi \qquad \overline{\Phi_n} = \frac{m_1 \operatorname{ctg} m_1 - m_2 \operatorname{ctg} m_2}{m_1^2 + m_2^2} \qquad (28)$$

$$\left.\frac{\partial w}{\partial y}\right|_{y=b} = -\frac{b}{D_y} \sum_n^\infty K_n \overline{\Psi_n} \sin n\pi\alpha\xi \qquad \overline{\Psi_n} = \frac{m_2 \operatorname{cosec} m_2 - m_1 \operatorname{cosec} m_1}{m_1^2 + m_2^2} \qquad (29)$$

Remarquons qu'à $\delta = 0$, c'est-à-dire $q = 0$, les grandeurs $\overline{\Phi}_n \to \Phi_n$, $\overline{\Psi}_n \to \Psi_n$.

Pour encastrer rigidement la plaque en l'arête $y=0$, nous obtiendrons de la condition $\left.\frac{\partial w}{\partial y}\right|_{y=0} = 0$ l'équation du flambage de la plaque $\overline{\Phi}_n = 0$.

Cette équation $m_1 \operatorname{ctg} m_1 = m_2 \operatorname{ctg} m_2$, ainsi que les relations (27a) vont nous déterminer ∞ la quantité infinie des racines δ.

II. Revenant au flambage de la plaque continue nous adopterons à $q > q_k$ les moments $M_y^r(x, 0)$ comme valeurs supplémentaires du système. La condition de continuité de la plaque aux appuis donne

$$-\left.\frac{\partial w^r}{\partial y}\right|_{y=br} + \left.\frac{\partial w^{r+1}}{\partial y}\right|_{y=0} = 0$$

Nous obtiendrons le système d'équations homogènes

$$K_n^{r-1}\beta^r\overline{\Psi}_n^r + K_n^r(\beta^r\overline{\Phi}_n^r + \beta^{r+1}\overline{\Phi}_n^{r+1}) + K_n^{r+1}\beta^{r+1}\overline{\Psi}_n^{r+1} = 0$$

$$(r=1, 2, \ldots, z-1), \qquad (n=1, 2, \ldots, \infty). \tag{30}$$

$$\beta^r = \frac{D_y^0 b_r}{D_y^r b^0}.$$

Nous poserons autant d'équations (30) qu'il y a de grandeurs inconnues des moments d'appui. Ce système sera non contradictoire, lorsque le déterminant du système d'équations $\Delta(\delta)$ sera égal à zéro.

Cette dernière condition ainsi que les relations (27a) établissent le critère du flambage de la plaque.

L'équation (30) comprend une série de cas particuliers.

a) Plaque librement appuyée sur ses arêtes $r-1$, $r+1$

$$K_n^{r-1} = K_n^{r+1} = 0, \qquad \Delta(\delta) = \beta^r\overline{\Phi}_n^r + \beta^{r+1}\overline{\Phi}_n^{r+1} = 0.$$

b) Plaque encastrée rigidement le long des arêtes r, $r+1$.

Dans l'équation (30) il faut poser

$$K_n^{r-1} = K_n^{r} = K_n, \qquad \beta^{r+1} = 0, \qquad \Delta(\delta) = \overline{\Phi}_n + \overline{\Psi}_n = 0.$$

Dans le cas particulier $b \longrightarrow \infty$ nous obtiendrons $q_k = \frac{\pi^2 D_x n^2}{a^2}$.

c) Plaque continue aux valeurs équivalentes de q, b, ρ dans toutes les aires avec le nombre d'appuis $z+1$.

En traitant l'équation

$$K_n^{r-1} + \bar{c}K_n^r + K_n^{r+1} = 0$$

$$(r=1, 2, \ldots, z-1)$$

$$\bar{c} = \frac{\overline{\Phi}_n}{\overline{\Psi}_n}$$

comme équation linéaire aux différences du second ordre avec solution $K_n^r = A_n \cos ar + B_n \sin ar$; en tenant compte des conditions des bords

($K_n^0 = 0$, $K_n^z = 0$) nous amènerons la condition du flambage de la plaque à l'expression

$$\cos \frac{\pi}{z} = \frac{\overline{\Phi}}{\overline{\Psi}}$$

ce qui, pour une quantité infinie de travées, donne $\overline{\Phi} = \overline{\Psi}$, ou bien

$$m_1 \operatorname{ctg} \frac{m_1}{2} = m_2 \operatorname{ctg} \frac{m_2}{2} .$$

Résumé

Ce mémoire présente un critère de flambage d'une plaque continue orthotrope librement appuyée sur son périmètre et sollicité par une charge uniformément répartie sur ses arêtes $x = 0$ et $x = a$.

Zusammenfassung

Es wurde für eine gleichmässig verteilte, in der Plattenmittelebene an den Rändern $x = 0$ und $x = a$ angreifende Kraft ein allgemeines Beulungskriterium für die orthotrope, durchlaufende, an den gleichen Rändern frei aufliegende Platte ermittelt.

Summary

This work presents the general solution of a continuous orthotropic plate whose edges ($x = 0$ and $x = a$) are loaded with $p = \text{const.}$ and freely supported on its perimeter.